Available online at www.sciencedirect.com

ScienceDirect

Procedia Engineering 207 (2017) 2298–2303

Procedia Engineering

www.elsevier.com/locate/procedia

International Conference on the Technology of Plasticity, ICTP 2017, 17-22 September 2017, Cambridge, United Kingdom

Quantitative analysis of galling in cold forging of a commercial Al-Mg-Si alloy

K. Le Mercier[a], M. Dubar[a,*], K. Mocellin[b], A. Dubois[a], L. Dubar[a]

[a]*UVHC, LAMIH UMR CNRS 8201, F-59313 Valenciennes, France.*
[b]*Mines PariTech, PSL – Research University, CEMEF – Centre for Material Forming, UMR CNRS 7635, F-06904 Sophia Antipolis, France.*

Abstract

Multiple upsetting-sliding tests are performed at sliding velocities in the range of 20-200 $mm.s^{-1}$ and at different plastic deformations to reproduce the local contact conditions experienced at the tool/workpiece interface during cold forging of a 6082 aluminium alloy. An original approach, able to evaluate accurately the volume of galled aluminium by means of surface topography acquisitions and energy dispersive spectrometry analyses, is presented. Galling is observed whatever the testing conditions and two types of regimes are underlined according to the sliding velocity. An interesting and strong correlation between the wear volumes and the friction ratio is also highlighted.

© 2017 The Authors. Published by Elsevier Ltd.
Peer-review under responsibility of the scientific committee of the International Conference on the Technology of Plasticity.

Keywords: AA6082, Wear, Galling, Upsetting Sliding Test, Surface topography.

1. Introduction

Cold forging is a suitable process for manufacturing near net shape components with a high production rate [1]. This forming process is performed at room temperature and produces precise parts with an excellent surface finish and enhanced mechanical properties, due to work-hardening. This process allows considerable savings in material,

* Corresponding author. Tel.: +33 3 27 51 13 91
E-mail address: mirentxu.dubar@univ-valenciennes.fr

1877-7058 © 2017 The Authors. Published by Elsevier Ltd.
Peer-review under responsibility of the scientific committee of the International Conference on the Technology of Plasticity.
10.1016/j.proeng.2017.10.998

machining and energy. Over the past few years, the use of cold forged aluminium alloys components has increased in a large variety of industrial applications, especially in the automotive field [2]. Indeed, aluminium alloys provide an efficient compromise between specific mechanical strength and corrosion resistance. However, processing of aluminium billets could give rise to adhesive wear [3]. Thus, the material which adheres on the tool surface is hardened by oxidation, work-hardening or grain refinement during the repeated forming cycles. Finally, the tool geometry is altered, the surface roughness is increased and scratches appear on the formed parts. This phenomenon, which compromises the process viability, is called galling. Usually, surface lubrication is used to improve the galling resistance of cold forging tools. The tool surface preparation, which governs the roughness parameters and topography, is also required to reduce the work material adhesion. In some cases, diamond like carbon (DLC) or hard ceramic coatings, which have a valuable impact on the reduction of this wear, are applied to the tool surface [4]. A recent experimental investigation, performed by Heinrichs et al. [5,8], allowed a better understanding of the galling mechanisms involved during the cold forging of aluminium. The initial transfer of aluminium was examined as a function of the surface roughness [5], coating material [6] and surface defects [7]. This investigation revealed that the immediate transfer of aluminium from an unlubricated billet cannot be avoided, irrespective of the surface roughness of the tool. Thus, the galling mechanism has a statistically significant likelihood of occurring when the lubricant is scraped off. Furthermore, the tool surfaces exhibited the same severe galling mechanism, irrespective of their composition. Finally, the study of Heinrichs et al. [8] highlighted the beneficial impact of DLC coatings, which cannot substitute the use of lubricants, on the galling resistance of cold forging tools. Other studies provided some explanations concerning the evolution of the galling mechanism at different temperatures. In the case of cold forging operations, the amount of galled aluminium, which increases with the sliding distance and not necessarily with the friction coefficient, is mainly induced by the surface topography of the tool [9, 10].

Thus, the present communication reports the main findings of an experimental investigation that has been conducted in order to analyse the galling mechanism during the cold forging of a 6082 aluminium alloy. This analysis has been carried out by means of upsetting-sliding tests (UST). This test is able to reproduce the local contact conditions experienced at the tool/workpiece interface such as contact pressure, sliding velocity and interface temperature. To evaluate the amount of galled material on the tool surfaces, an original specific approach based on the combination of surface topography acquisitions and energy dispersive spectrometry analyses is introduced.

2. Experimental procedure

2.1. Upsetting sliding test (UST)

The wear tests were conducted under upsetting sliding conditions, which allows the investigation of tribological characteristics of cold forging processes. This specific test is able to reproduce the local conditions of contact experienced at the tool/workpiece interface such as contact pressure, sliding velocity and interface temperature [11-13]. The lubricant efficiency can also be investigated by means of this device.

Before the beginning of the test, a round billet of an AA6082-T6 aluminium alloy is clamped in a fixed stand as illustrated in Fig. 1. A normal displacement is applied between the top of the tool and the round billet surface. During the friction test, the tool, which is made of a X38CrMoV5-3 tool steel, slides along the round billet, at a constant velocity. This generates a locally deformed area on the specimen surface. The UST device, which is exhibited in Fig. 1a, includes two load cells for measuring both normal and tangential forces resulting from the compression of the billet and friction at the tool/specimen interface. The tools have a cylindrical shape of 20 mm in radius. Each tool surface was polished with a 1000-grit SiC paper. The specimens were cylindrical samples of 50 mm in height and 15 mm in diameter. A bevelled edge was machined at their base to avoid a rough initial contact with the tool. The tests were performed at room temperature, at mean speeds of 20, 100 and 200 $mm.s^{-1}$ and at different aimed normal displacements which are reported in Tab. 1. The billets were lubricated with a solid film of molybdenum disulphide (MoS_2). Each test configuration was performed three times with a single tool in contact with an unworn billet surface, which results in an effective sliding distance of 150 mm.

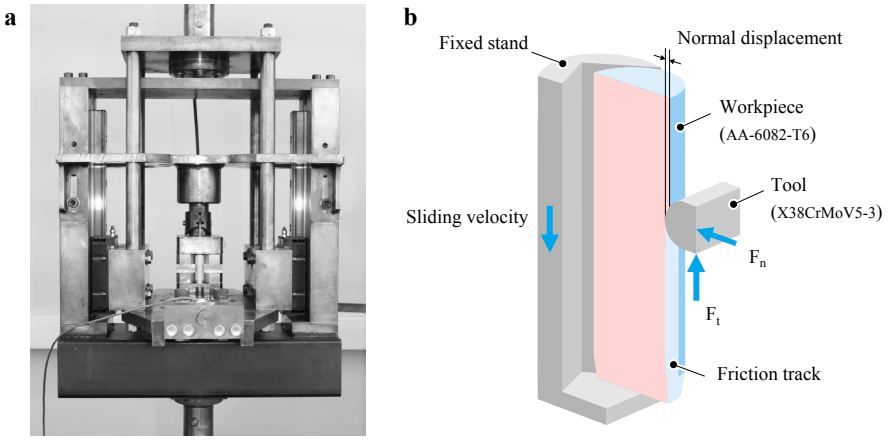


Fig. 1. (a) Upsetting sliding test device; (b) Schematic diagram of the test.

Table 1. Tested configurations.

Tool/Test configuration	1	2	3	4	5	6	7	8	9	10
Sliding velocity (mm.s^{-1})	20	20	20	100	100	100	200	200	200	200
Normal displacement (µm)	30	60	100	30	60	100	30	40	60	100

2.2. Surface analysis procedure

With the aim of understanding the material transfer controlling mechanisms, an efficient approach is to couple scanning electron microscopy (SEM) and surface profilometry [14]. Therefore, the contact surface of each tool was analysed after the UST evaluation. Surface profilometry was performed by means of the MesRug 3D massive surface topography acquisition tool [15]. Surface topography data were obtained using a three-dimensional non-contact optical profilometer (Zygo NewView^{TM} 7300, Zygo Corp.,USA). The white-light interferometer was used with a x20 Mirau objective. Small surfaces of 349 x 262 squared microns were measured individually. Using the stitching function, they were overlapped 20 percent to obtain a large surface of 9.5 x 5.5 mm², which is described by 17536 x 10848 points. SEM observations were carried out on the worn surface of the tools, by means of a FEI Quanta^{TM} 400 scanning electron microscope. Energy dispersive spectroscopy (EDS) analyses were also carried out.

3. Experimental results and discussion

3.1. Analysis of the UST results

Representative normal and tangential forces of the third test configuration (see Tab. 1) are reported in Fig. 2a. The results of a single test are represented by dashed curves whereas the solid lines correspond to the average of three tests. Thus, it can be clearly observed that the UST is quite reproducible. The increase of both forces observed before a sliding distance of 5 mm corresponds to the initial contact between the tool and the bevelled edge of the billet. A plateau is then achieved until a sliding distance of 45 mm. Finally, when the tool moves away from the workpiece, a marked decrease in both normal and tangential forces is observed. The contact pressure can be determined by means of a finite element model developed on the basis of Brocail et al. works [16]. For this third test configuration, the mean contact pressure is around 433 MPa and the contact area is around 10.33 mm².

Fig. 2b illustrates the values of the mean friction ratio F_t/F_n for each UST configuration. At low sliding velocities, the values of this ratio are higher than those observed at higher sliding speeds. The influence of the effective normal

displacement is only noticeable at high sliding velocities. Indeed, as the normal displacement increases, the friction ratio also increases. However, this trend has not been observed for a sliding velocity of 20 mm.s^{-1}.

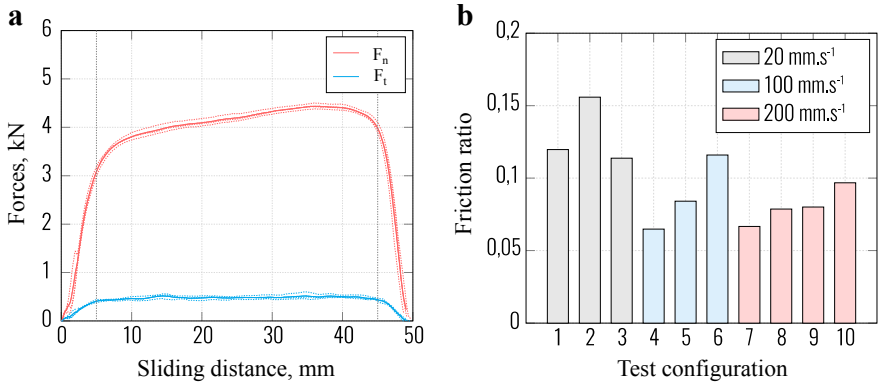


Fig. 2. (a) Normal and tangential forces of the third UST configuration; (b) Mean friction ratio of each UST configuration.

3.2. Analysis of the galling mechanisms

The evaluation of aluminium alloy volume transferred to the tools surfaces is performed after conducting three tests, which corresponds to a sliding distance of 150 mm. Firstly, EDS analyses are carried out to determine the shape of the worn areas by discerning the aluminium (red) from the iron (blue). Fig. 3a illustrates the EDS analysis of the third tool. Thereafter, a specific post-processing methodology is applied to the surface topography acquisition (Fig. 3b). White dashed lines can be distinguished in the centre representing the transferred aluminium. From this rough acquisition, it's not possible to correctly quantify the transferred volume. So, the first step consists in removing the initial shapes of the tools. As the surface of the tool is not perfectly cylindrical, the surface topography acquisitions are flattened out by means of a 7th degree polynomial without considering the worn area (Fig. 3c). Fig. 3d illustrates the resultant surface topography acquisition of the third tool. The worn area can be divided in two regions: the contact upstream, where most of the transferred work material is located and the contact downstream corresponding to a residual deposit.

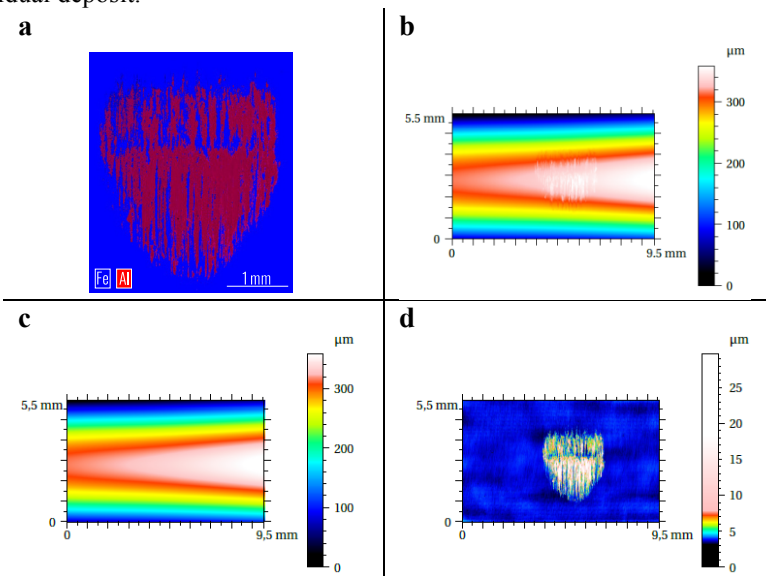


Fig. 3. (a) EDS analysis of the third tool; (b) Original surface topography acquisition; (c) 7th degree polynomial surface subtracted; (d) Resultant surface topography acquisition.

The second step consists in the evaluation of the amount of work material adhesion by measuring the peaks volumes. Nevertheless, a specific thresholding had to be performed to extract the core roughness from the flattened surface. This was performed by means of the material ratio curve which was computed as indicated in the ISO 13565-2 [17]. Fig. 4a illustrates the material ratio curve corresponding to the surface topography shown in Fig. 3b. The Mr_1 parameter, which is defined as the material ratio determined for the intersection line which separates the protruding peaks from the roughness core profile in the ISO 13565-2, is used as a threshold. Fig. 4b exhibits the surface topography reduced to a 5 mm square after the Mr_1 thresholding. The worn area is clearly highlighted. The wear volumes are computed by the MesRug software with its islands detection module. Fig. 4b illustrates the wear volumes of each test configurations. The wear volumes follow the same trends as those observed for the friction ratio (see Fig 2b). Indeed, the wear volumes of the first two configurations are higher than those observed at higher sliding speeds and the influence of the effective normal displacement is also noticeable at high sliding velocities.

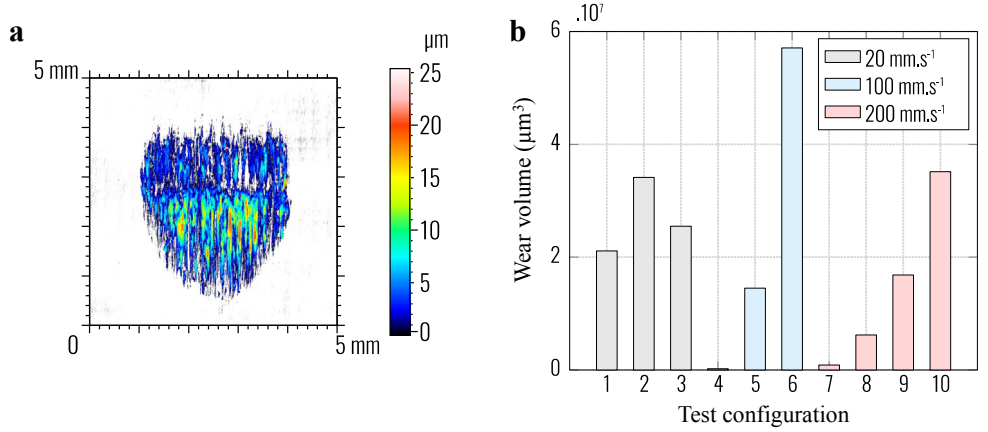


Fig. 4. (a) Surface topography after the thresholding; (b) Wear volumes evaluated of each test configuration.

The following graphs show the wear volume as a function of the friction ratio obtained for the three sliding velocities (Fig. 5). A strong correlation between the friction ratio and the wear volumes is observed. Moreover, the linear regressions highlight two types of galling regime according to the sliding velocity. At 100 and 200 $mm.s^{-1}$, the linear regression coefficients are very close, which suggests that the same galling mechanism is observed. At the lowest velocity, the wear volumes do not follow the same regression, which underlines that another regime is taking place.

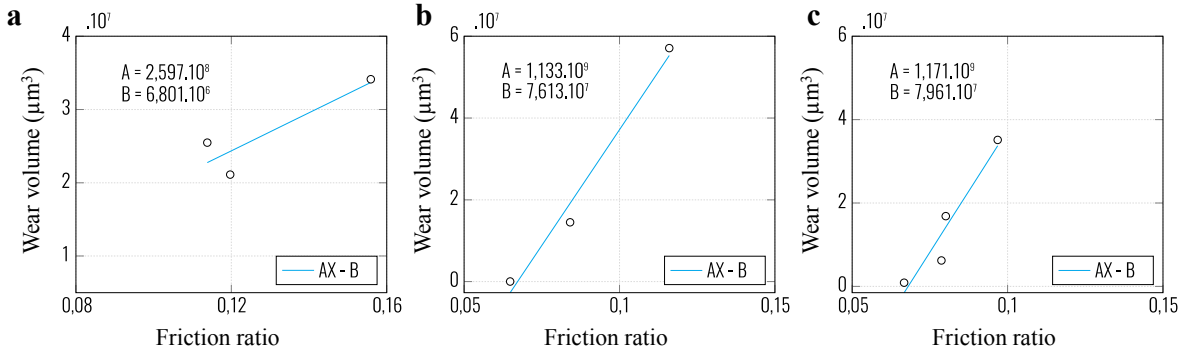


Fig. 5. Wear volumes as a function of the friction ratio (a) 20 $mm.s^{-1}$ (b) 100 $mm.s^{-1}$ (c) 200 $mm.s^{-1}$.

4. Conclusions

Galling has been observed whatever the testing conditions and two types of galling regime have been underlined according to the sliding velocity. A specific approach, which combines surface profilometry and scanning electron microscopy, has been proposed for the evaluation of galled volumes. Moreover, an interesting and strong correlation between the wear volumes and the friction ratio has been highlighted, showing the importance of taking into account a parameter representing friction in adhesive wear models, such as those developed by means of an energy approach based on the interfacial shear work. Finally, in order to provide a better analytical understanding of the adhesion mechanisms involved in these tests, a finite element model has to be developed. This model will allow the evaluation of the local contact pressures and sliding velocities experienced at the tool/workpiece interface. Also, a wear model could be developed by means of this numerical simulation.

Acknowledgements

The present research work has been supported by the Hauts de France Regional Council, the European Community, the Ministry of Higher Education and Research, the Carnot ARTS institute and the National Center for Scientific Research. The authors gratefully acknowledge the support of these institutions. They also express their sincere thanks to Dr. J. Bouquerel (Associate Professor, UMET) for the SEM observations, R. Deltombe (Research Engineer, LAMIH) for the surface topography acquisitions and B. Laurent (Manufacturing workshop manager, LAMIH) for his valuable technical support.

References

[1] T. Altan, G. Ngaile, G. Shen, Cold and hot forging: fundamentals and applications, Vol.1, ASM International, 2005.
[2] N. Bay, Cold forming of aluminium - State of the art, Journal of Materials Processing Technology,Vol.71, n°1, 1997, pp. 76-90.
[3] P. Groche, G. Nitzsche, Influence of temperature on the initiation of adhesive wear with respect to deep drawing of aluminium-alloys, Journal of Materials Processing Technology, Vol.191, n°1-3, 2007, pp. 314-316.
[4] B. Podgornik, J. Jerina, Surface topography effect on galling resistance of coated and uncoated tool steel, Surface and Coatings Technology, Vol.206, n°11-12, 2012, pp. 2792-2800.
[5] J. Heinrichs, S. Jacobson, Laboratory test simulation of galling in cold forming of aluminium, Wear, Vol. 267, n°12, 2009, pp. 2278-2286.
[6] J. Heinrichs, S. Jacobson, Laboratory test simulation of aluminium cold forming - influence from PVD tool coatings on the tendency to galling, Surface and Coatings Technology, Vol. 204, n° 21-22, 2010, pp. 3606-3613.
[7] J. Heinrichs, S. Jacobson, The influuence from shape and size of tool surface defects on the occurrence of galling in cold forming of aluminium, Wear, Vol.271, n° 9-10, 2011, pp. 2517-2524.
[8] J. Heinrichs, M. Olsson, S. Jacobson, Mechanisms of material transfer studied in situ in the SEM: Explanations to the success of DLC coated tools in aluminium forming, Wear, Vol. 292-293, 2012, pp.49-60.
[9] J. Pujante, L. Pelcastre, M. Vilaseca, D. Casellas, B. Prakash, Investigations into wear and galling mechanism of aluminium alloy-tool steel tribopair at different temperatures, Wear, Vol. 308, n° 1-2, 2013, pp.193-198.
[10] J. Jerina, M. Kalin, Initiation and evolution of the aluminium-alloy transfer on hot-work tool steel at temperatures from 20°C to 500°C, Wear, Vol. 319, n° 1-2, 2014, pp. 234-244.
[11] M. Dubar, A. Dubois, L. Dubar, Wear analysis of tools in cold forging: PVD versus CVD TiN coatings, Wear, Vol. 259, n° 7-12, 2005, pp. 1109-1116, 15th International Conference on Wear of Materials.
[12] A. Dubois, M. Dubar, L. Dubar, Warm and Hot Upsetting Sliding Test: Tribology of Metal Processes at High Temperature, Procedia Engineering, Vol. 81, 2014, pp. 1964-1969, 11th International Conference on Technology of Plasticity, ICTP 2014, 19-24 October 2014, Nagoya Congress Center, Nagoya, Japan.
[13] J. Bouquerel, B. Diawara, A. Dubois, M. Dubar, J. B. Vogt, D. Najjar, Investigations of the microstructural response to a cold forging process of the 6082-T6 alloy, Materials & Design, Vol. 68, 2015, pp. 245-258.
[14] N. S. Nosar, M. Olsson, Influence of tool steel surface topography on adhesion and material transfer in stainless steel/tool steel sliding contact, Wear, Vol. 303, n° 1-2, 2013, pp. 30-39.
[15] R. Deltombe, K. J. Kubiak, M. Bigerelle, How to select the most relevant 3D roughness parameters of a surface, Scanning, Vol. 36, n°1, 2014, pp. 150-160.
[16] J. Brocail, M. Watremez, L. Dubar, Identification of a friction model for modelling of orthogonal cutting, International Journal of Machine Tools and Manufacture, vol. 50, n° 9, 2010, pp. 807 – 814.
[17] ISO/TS 13565-2, Geometrical product specifications (GPS) - Surface method: Profile method, Surfaces having stratified functional properties - Part 2: Height characterization using the linear material ratio curve, International Organization for Standardization.